

BEAM DYNAMICS IN AN ELECTRON LENS WITH THE WARP PARTICLE-IN-CELL CODE*

G. Stancari[†], Fermilab, Batavia, IL 60510, USA, S. Redaelli, CERN, Geneva, Switzerland
V. Moens, EPFL, Lausanne, Switzerland

Abstract

Electron lenses are a mature technique for beam manipulation in colliders and storage rings. In an electron lens, a pulsed, magnetically confined electron beam with a given current-density profile interacts with the circulating beam to obtain the desired effect. Electron lenses were used in the Fermilab Tevatron collider for beam-beam compensation, for abort-gap clearing, and for halo scraping. They will be used in RHIC at BNL for head-on beam-beam compensation, and their application to the Large Hadron Collider for halo control is under development. At Fermilab, electron lenses will be implemented as lattice elements for nonlinear integrable optics. The design of electron lenses requires tools to calculate the kicks and wakefields experienced by the circulating beam. We use the Warp particle-in-cell code to study generation, transport, and evolution of the electron beam. For the first time, a fully 3-dimensional code is used for this purpose.

INTRODUCTION

Electron lenses are pulsed, magnetically confined, low-energy electron beams whose electromagnetic fields are used for active manipulation of the circulating beam in high-energy accelerators [1, 2] (Figure 1). The first main feature of an electron lens is the possibility to control the current-density profile of the electron beam (flat, Gaussian, hollow, etc.) by shaping the cathode and the extraction electrodes. Another feature is pulsed operation, enabled by the availability of high-voltage modulators with fast rise times. The electron beam can therefore be synchronized with subsets of bunches, with different intensities for each subset. The main advantage of the use of electron lenses for high-power accelerators is the absence of metal close to the beam, therefore avoiding material damage and impedance.

Electron lenses were developed for beam-beam compensation in colliders [3], enabling the first observation of long-range beam-beam compensation effects by tune shifting individual bunches [4]. They were used for many years during regular Tevatron collider operations for cleaning uncaptured particles from the abort gap [5]. Thanks to the reliability of the hardware, one of the two Tevatron electron lenses could be used for experiments on head-on beam-beam compensation in 2009 [6], and for exploring hollow electron beam

collimation in 2010–2011 [7, 8]. Electron lenses for beam-beam compensation were built for the Relativistic Heavy Ion Collider (RHIC) at Brookhaven National Laboratory and are being commissioned [9, 10]. Current areas of research on electron lenses include the generation of nonlinear integrable lattices in the Fermilab Integrable Optics Test Accelerator (IOTA) [11, 12] and applications for the LHC upgrades: as halo monitors and scrapers [7, 13], and as charged current-carrying ‘wires’ for long-range beam-beam compensation [14].

Because the electron beam is strongly magnetized, the center of gyration of the electron trajectories follows the magnetic field lines with good approximation. So far, both the Tevatron and the RHIC electron lenses were designed with this assumption, using single-particle dynamics. The wide range of new applications being proposed poses different requirements on beam intensity and on the symmetry of the current-density profiles. The Warp particle-in-cell code [15] was chosen to evaluate the effects of the electron lens imperfections and the space-charge evolution of the electron beam at high intensities.

MOTIVATION

The main goals of the numerical simulations are the following:

- to evaluate the effects of imperfections and asymmetries in the transport system on the quality of the beam profile.
- to estimate the effects of the toroidal injection and extraction bends on the dynamics of the circulating beam.

Both of the above items apply to all electron-lens applications:

- to calculate the azimuthal evolution of the profiles under space charge. This is particularly important for hollow electron beam collimation, where the electric field on axis should be as small as possible.

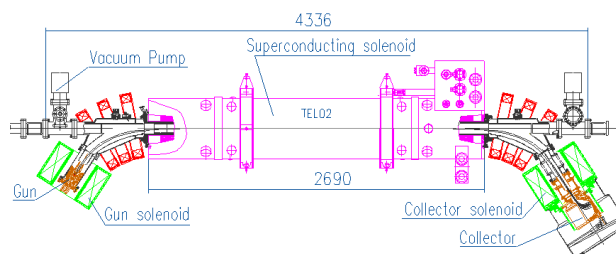


Figure 1: Layout of a Tevatron electron lens (dimensions in millimeters).

* Fermilab is operated by Fermi Research Alliance, LLC under Contract No. DE-AC02-07CH11359 with the United States Department of Energy. This work was partially supported by the US DOE LHC Accelerator Research Program (LARP) and by the European FP7 HiLumi LHC Design Study, Grant Agreement 284404. Report number: FERMILAB-CONF-14-180-APC.

[†] Email: stancari@fnal.gov

Content from this work may be used under the terms of the CC BY 3.0 licence (© 2014). Any distribution of this work must maintain attribution to the author(s), title of the work, publisher, and DOI.

- to investigate the stability of the system at the very high currents (about 20 A) required for long-range beam-beam compensation for the LHC upgrades or at low fields (0.4 T with a resistive main solenoid) in the Fermilab Integrable Optics Test Accelerator.

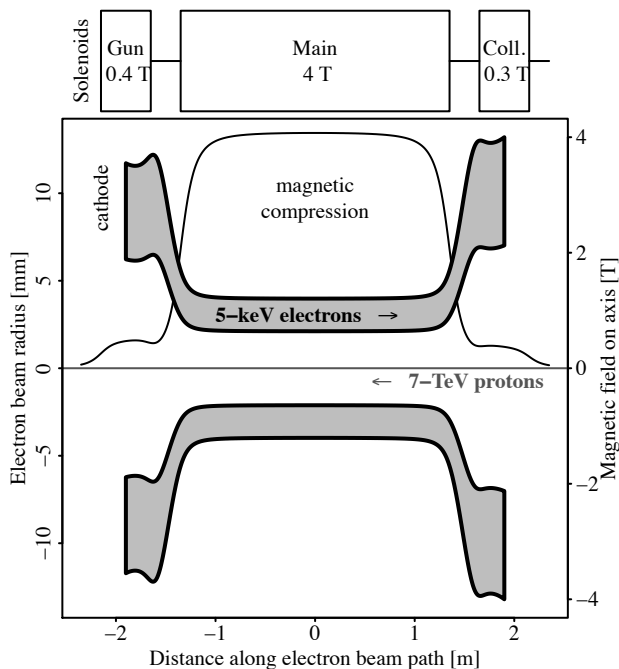


Figure 2: Schematic layout of hollow electron beams for halo scraping.

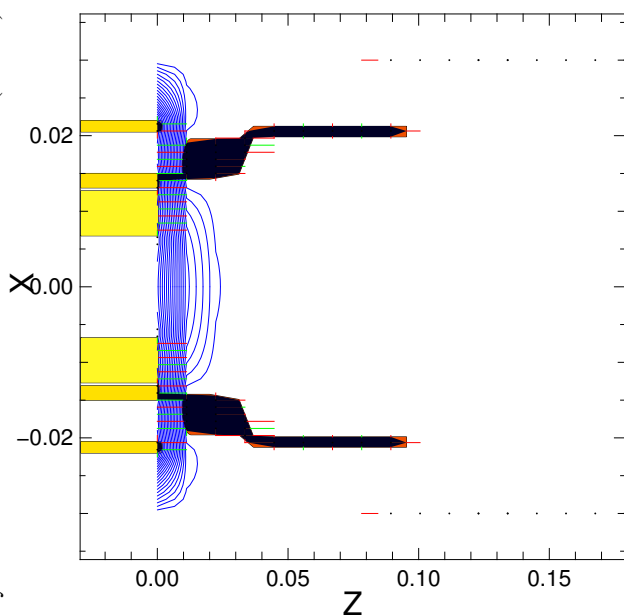


Figure 3: Warp implementation of an axially symmetric hollow electron gun. The longitudinal coordinate Z and the horizontal coordinate X are expressed in meters. One can see the outline of the cathode and extraction electrodes (yellow and black surfaces), and the equipotential lines (in blue).

In an electron lens, toroidal bends are used for injecting and extracting the electron beam (Figure 1). The curved charge distribution of electrons may have an effect on the dynamics of the circulating beam. A simplified calculation of the kick maps was presented in Refs. [16, 17] and then used in numerical tracking simulations for the LHC [18].

Figure 2 shows the layout of the beams for proton halo scraping in the LHC. If the electron distribution is axially symmetric, the proton beam core is unperturbed, whereas the halo experiences smooth and tunable nonlinear transverse kicks. Two-dimensional azimuthal asymmetries of the electron current density in the overlap region inside the main solenoid may be caused by the space-charge evolution of the hollow electron beam as it propagates through the electron lens, or by imperfections in the electron gun geometry, magnetic field lines, etc.

METHODS

There are several electron-lens configurations of interest:

- a straight geometry with resistive solenoids, similar to the Fermilab electron-lens test stand, where current-density profiles can be measured under different conditions and compared with simulations.
- bent geometries. These can be C-shaped (with gun and collector on the same side of the ring), as in the Tevatron and RHIC electron lenses; or S-shaped (with gun and collector on opposite sides of the ring to cancel dipole kicks on the circulating beam), which will be more appropriate for the LHC or IOTA.

The electron beam can be injected with a given distribution or generated by the thermionic cathode in the space-charge-limited regime. Figure 3 shows the Warp implementation of the hollow electron gun that was built at Fermilab

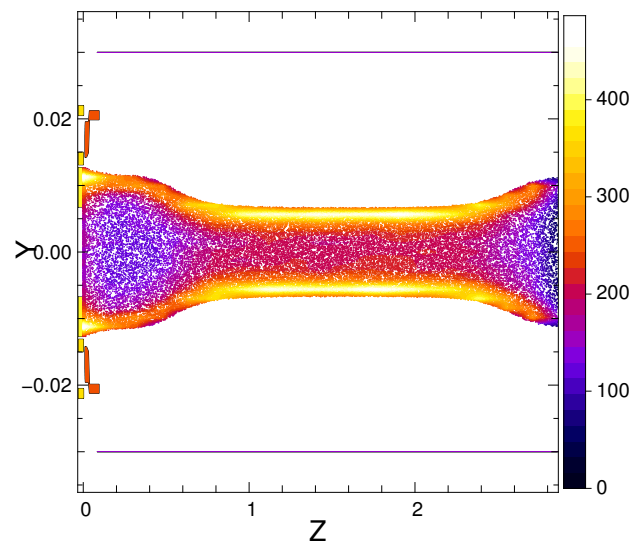


Figure 4: Particle distribution at the end of propagation through the electron lens test stand. The longitudinal coordinate Z and the vertical coordinate Y are expressed in meters.

as a prototype for the LHC [19, 20]. This gun can yield a peak current of 5 A at 10 kV.

For tests, Warp is run on Linux laptops or other Fermilab multicore machines. Production calculations are run on the Fermilab Accelerator Simulations Wilson Cluster [21], as described in Ref. [22].

Figure 4 shows an example of the macroparticle distribution after the 5-keV electrons propagate through the 2.8 m of the electron-lens test stand. The axial fields were 0.1 T in the gun, 0.4 T in the main solenoid, and 0.1 T in the collector. One can see the magnetic compression of the hollow electron beam in the central part of the device.

CONCLUSIONS

Electron lenses were implemented in the Warp particle-in-cell code for the first time, to aid in the 3-dimensional design of these devices for a wide range of applications in circular accelerators. At this stage, mostly technical issues were addressed: managing of computational resources, memory in particular; the implementation of particle injection from measured current-density profiles; and the bends in the electron lens configuration. For the straight geometries, field maps and density profiles were obtained, which will then be used for comparisons with measurements and as inputs for numerical tracking.

ACKNOWLEDGMENTS

The authors would like to thank in particular D. Grote (LLNL) for his invaluable help on the Warp code, A. Singh and E. Stern (Fermilab) for their support on the Fermilab Accelerator Simulations Cluster, M. Chung (Fermilab) for his insights on nonneutral plasma physics simulations, and A. Valishev (Fermilab) for his advice on numerical simulations and on the physics of electron lenses. This work was conducted as part of a joint master thesis with EPFL, CERN, and Fermilab, coordinated by Prof. L. Rivkin.

REFERENCES

- [1] V. Shiltsev et al., Phys. Rev. ST Accel. Beams **11**, 103501 (2008).
- [2] V. Shiltsev in *Handbook of Accelerator Physics and Engineering*, edited by A. W. Chao, K. H. Mess, M. Tigner, and F. Zimmermann (2nd ed., World Scientific, 2013), p. 641.
- [3] V. Shiltsev et al., Phys. Rev. ST Accel. Beams **2**, 071001 (1999); New J. Phys. **10**, 043042 (2008).
- [4] V. Shiltsev et al., Phys. Rev. Lett. **99**, 244801 (2007).
- [5] X. Zhang et al. Phys. Rev. ST Accel. Beams **11**, 051002 (2008).
- [6] G. Stancari and A. Valishev, in Proceedings of the ICFA Workshop on Beam-Beam Effects in Hadron Colliders (BB2013), Geneva, Switzerland, March 2013, FERMILAB-CONF-13-046-APC.
- [7] G. Stancari et al., Phys. Rev. Lett. **107**, 084802 (2011).

- [8] G. Stancari, in Proceedings of the Meeting of the Division of Particles and Fields of the American Physical Society, Providence, RI, USA, August 2011, arXiv:1110.0144 [physics.acc-ph], FERMILAB-CONF-11-506-AD-APC.
- [9] W. Fischer et al., in Proceedings of the 2013 International Particle Accelerator Conference (IPAC13), Shanghai, China, May 2013, p. 1526.
- [10] W. Fischer et al., in Proceedings of the 2014 International Particle Accelerator Conference (IPAC14), Dresden, Germany, June 2014, paper ID 1124 / TUYA01.
- [11] S. Nagaitsev et al., in Proceedings of the 2012 International Particle Accelerator Conference (IPAC12), New Orleans, LA, USA, May 2012, p. 16, FERMILAB-CONF-12-247-AD.
- [12] A. Valishev et al., in Proceedings of the 2012 International Particle Accelerator Conference (IPAC12), New Orleans, LA, USA, May 2012, p. 1371, FERMILAB-CONF-12-209-AD-APC.
- [13] G. Stancari et al., Conceptual design of hollow electron lenses for beam halo control in the Large Hadron Collider, FERMILAB-TM-2572-APC, arXiv:1405.2033 [physics.acc-ph] (May 2014).
- [14] A. Valishev and G. Stancari, Electron lens as beam-beam wire compensator in HL-LHC, FERMILAB-TM-2571-APC, arXiv:1312.1660 [physics.acc-ph] (November 2013).
- [15] J.-L. Vay, D. P. Grote, R. H. Cohen, and A. Friedman, Comput. Sci. Disc. **5**, 014019 (2012).
- [16] G. Stancari et al., in Proceedings of the 2013 North-American Particle Accelerator Conference (NA-PAC13), Pasadena, California, USA, September 2013, p. 481, FERMILAB-CONF-13-356-APC.
- [17] G. Stancari, Calculation of the transverse kicks generated by the bends of a hollow electron lens, FERMILAB-FN-0972-APC, arXiv:1403.6370 [physics.acc-ph] (February 2014).
- [18] A. Valishev, Simulation study of hollow electron beam collimation for LHC, FERMILAB-TM-2584-APC (May 2014).
- [19] S. Li and G. Stancari, FERMILAB-TM-2542-APC (August 2012).
- [20] V. Moens, Masters Thesis, École Polytechnique Fédérale de Lausanne (EPFL), Switzerland, FERMILAB-MASTERS-2013-02 and CERN-THESIS-2013-126 (August 2013).
- [21] K. Schumacher, A. Singh et al., The Accelerator Simulations Wilson Cluster, `tev.fnal.gov`
- [22] V. Moens, Guide for 3D Warp simulations of hollow electron beam lenses, FERMILAB-TM-2586-APC.